JOURNAL OF CATALYSIS 128, 293–302 (1991)

Amorphous $AlPO_4$ as Catalyst Support

2. Characterization of Amorphous Aluminum Phosphates[1]

BERND REBENSTORF,*,[2] THOMAS LINDBLAD,* AND S. LARS T. ANDERSSON†

*Research Group on Catalysis, Inorganic Chemistry 1, and †Chemical Technology, Chemical Center, University of Lund, Box 124, S-221 00 Lund, Sweden

Received March 22, 1990; revised August 20, 1990

Three different amorphous aluminum phosphates have been characterized by their specific surface area and pore volume and by XPS and FTIR studies. Three types of Al surface hydroxyl groups at 3793.8, 3768.5, and 3743.2 cm^{-1} and only one type of P surface hydroxyl groups at 3677.5 cm^{-1} are found in FTIR spectra after evacuation at 800°C. The ratio of the integrated absorbance of the IR bands from AlOH and POH surface groups is a sensitive tool to study the surface of $AlPO_4$ directly. A linear relation between the electronegativity of the metal ion and the stretching vibration of surface hydroxyl groups is proposed for Al, Si, P, and B tetrahedral surface ions. The three Al surface hydroxyl groups are assigned to four-coordinated (tetrahedral), five-coordinated, and six-coordinated surface Al ions. Amorphous $AlPO_4$ contains four- and five-coordinated Al ions and $AlPO_4$ with high specific surface area also has six-coordinated Al ions at the surface. CO is adsorbed on the phosphorus surface hydroxyl groups at low temperature, giving an IR band at 2170 cm^{-1}, while the IR band from the PO–H group is shifted to 3495 cm^{-1}. On $AlPO_4$ of high surface area, CO is also adsorbed on coordinatively unsaturated, five-coordinated Al surface ions. Four-coordinated Al ions are also found, but none with the coordination number three. Impregnation with chromium compounds in ethanol does not change the specific surface area, whereas impregnation in water resulted in a decreased specific surface area, to less than half of its previous value.

INTRODUCTION

Amorphous phosphates have found increasing interest as catalysts or catalyst supports in the last 30 years (*1*). Of these phosphates, aluminum phosphate is the one with the highest specific surface, which may be as large as 525 m^2/g (*1*). Such a value is comparable to those measured on silica gels, which are also amorphous. The basic building units are in both cases tetrahedral: for silica gel these are SiO_4 units, while in $AlPO_4$ two different types are involved, i.e., AlO_4 and PO_4 units. The Si–O distance in silica gel is 1.61 Å (*2*), while Al–O and P–O distances in amorphous $AlPO_4$ are 1.70 and 1.516 Å (*1*), respectively. Therefore silica gel and amorphous $AlPO_4$ are structurally very similar.

However, the surfaces of the two amorphous materials are very different. While silica gel has only slightly acidic surface silanol groups (*3*), which show an O–H stretching vibration for single surface hydroxyl groups at 3745 cm^{-1} (*3*), amorphous $AlPO_4$ has two different types of surface hydroxyl groups: AlOH and POH. The more acidic phosphorus surface hydroxyl groups have a stretching vibration at 3680 cm^{-1} and the more alkaline aluminum surface hydroxyl groups at 3800 cm^{-1} (*4*). One can therefore expect that the phosphorus surface hydroxyl groups will react more easily with cations than will the aluminum ones. Using these two amorphous materials as catalyst supports may therefore influence the catalytically active sites either by altering the

[1] For Part 1, see Ref. (*17*).

[2] To whom correspondence should be addressed.

0021-9517/91 $3.00

electron density on the surface (transition) metal atoms or by altering the geometry of the active sites.

Recently, amorphous aluminum phosphates with high pore volumes have been used as supports (*5–9*) for modifications of the Phillips catalyst (chromium(VI) on silica gel) (*10*) and the Union Carbide catalyst (chromocene on silica gel) (*11*) for the polymerization of ethylene.

The Union Carbide and the reduced Phillips catalysts have been studied previously in our laboratory using FTIR spectroscopy of CO adsorbed on the catalytically active chromium surface sites (*12–16*) as the principal investigation technique. The results can best be explained assuming dinuclear chromium surface compounds as the catalytically active sites.

At present our interest lies in investigating amorphous phosphates as catalyst supports, especially for the Phillips and Union Carbide catalysts (*17*). The present paper deals mainly with the characterization of these supports.

EXPERIMENTAL

Amorphous aluminum phosphates were prepared from $Al(NO_3)_3 \cdot 6H_2O$ and $(NH_4)_2HPO_4$. Two different P/Al ratios have been used: 1.1 (support **I**) and 0.9 (support **II**). The starting materials were dissolved in water acidified with HNO_3 and the hydrogel was formed by adding concentrated ammonia solution to a pH of 8. After 1 h the solvent was filtered off and the hydrogel washed with two times its volume of distilled water. The hydrogel was then dried at 120°C for 16 h and calcined at 500°C in air for 30 min. In addition, a high pore volume aluminum phosphate, SMR 9-1897 (from Grace, West Germany), was used (support **III**, also calcined at 500°C).

The three supports were impregnated with 0.5 wt% chromium in three different ways: (**A**) chromium(III) acetylacetonate in ethanol, (**B**) chromium(III) chloride (green) in ethanol, and (**C**) chromium (VI) oxide in water. The ethanol was removed by cautious heating of the samples to 80°C in air and calcination again at 500°C. The samples will be referred to below by the support number and the impregnation procedure, i.e., **IA** to **IIIC** (see also Table 1).

Surface areas were measured in a Micromeritics Flowsorb 2300 after degassing at 350°C for 2 h. For some samples the surface area was also measured in a gravimetric BET apparatus. These samples were degassed at 350°C for 18 h by evacuation to $<10^{-3}$ Pa. The error of the surface area measurements is ±5%. Pore size distributions were calculated from the desorption branch by the method of Dollimore and Heal (*18*).

X-ray diffractograms were obtained with a Philips PW 1710 powder diffraction unit equipped with a PW 1050 wide-angle goniometer and a LiF monochromator.

The XPS studies were performed on a Kratos XSAM 800 instrument. An Al anode (1486.6 eV) was used. The slitwidths were set at 40° and the analyzer was operated at a 40-eV pass energy and at high magnification. Charging effects were corrected for by adjusting the main C 1*s* peak to a position at 285.0 eV. Analysis of the spectra was performed with the DS 800 data system. Sensitivity factors used in the quantification were O 1*s* = 0.66, Al 2*p* = 0.19, and Cr 2*p* = 2.30 as supplied by Kratos, whereas P 2*p* = 0.434 was obtained from the known composition of support **I** (P/Al, 1.1) and support **II** (P/Al, 0.9).

The IR spectra were recorded on a Nicolet 20 SXC FTIR spectrometer with a resolution of 2 cm^{-1} and 1024 scans were averaged.

The IR cell has been described previously (*19*). A self-supporting disk (65 mg; diameter, 2 cm) of the sample was heated in an IR cell to 800°C under vacuum. At 500 and 800°C the sample was treated with oxygen (1 atm) for 10 min each. Thereafter CO was added at 350°C (15 min). The CO was evacuated at 300°C and a spectrum was recorded at room temperature. The cell was filled with 10 kPa CO and spectra were recorded at room temperature and at −85 and −115°C

TABLE 1

Surface Areas ($m^2\ g^{-1}$) of Various $AlPO_4$ Samples Measured with Flowsorb 2300 Equipment

Support	Type of impregnation			
	None	$Cr(acac)_3$ ethanol	$Cr((H_2O)_4Cl_2)Cl$ ethanol	CrO_3 water
I	132	140	129	43
II	145	137	143	74
III	287	297	296	136
Impregnation code		**A**	**B**	**C**

(100 Pa CO). This standard procedure was changed if necessary as indicated in the text below.

The CO IR spectra are always difference spectra, calculated by subtracting the first IR spectrum of each sample (after evacuation at 300°C) from the other ones. The fringes in Fig. 8, spectra 1 and 2, are due to incomplete subtraction of the gas-phase spectrum of CO. This incomplete subtraction arises from small wavenumber shifts in the spectra, caused by a shift in the laser frequency, which calibrates the interferograms. Variations in the optical thickness of different sample disks may be the ultimate cause.

RESULTS

Surface Areas

The BET surface areas are shown in Table 1. Of the two supports **I** and **II,** prepared in the same way, a slightly larger area is observed for the latter, having a P/Al ratio of 0.9. Impregnation with chromium compounds in ethanol solution hardly affects these surface areas. Taking the mean values of the three preparations of support **I** and of support **II** (**I, IA, IB** and **II, IIA, IIB**) gives surface areas of 134 and 142 m^2/g, respectively. Impregnation with CrO_3 in water solution, on the other hand, results in a large reduction of the surface area. The commercial $AlPO_4$ (Grace) gave a much larger surface area, 287 m^2/g, which did not change upon impregnation in ethanol. As for the other carriers, impregnation in water solution resulted in a large reduction of the surface area.

Table 2 shows pore volume, cumulative surface area, and BET surface area as measured in the gravimetric BET apparatus. A comparison of these surface areas with those reported in Table 1 shows a reasonable agreement for samples **I, II,** and **IIIC.** For sample **III,** having a much higher surface area, a large discrepancy in the surface area obtained by the two methods is observed. The reason for this behavior may be that the outgassing condition in the Flowsorb (outgassing in a flow of dry He at 350°C for 2 h) is too mild compared to the outgassing at 350°C for 18 h with pumping down to a vacuum $<10^{-3}$ Pa as in the gravimetric equipment.

The pore volume (Table 2) is of a size adequate for a commercial ethylene polymerization catalyst (1–1.5 cm^3/g) only for support **III.** The large reduction in surface area on impregnation with chromium salts in water solution for sample **IIIC** has also resulted in a large reduction in the pore volume, to a size similar to that for the other supports. The cumulative pore volume versus the pore diameter is shown in Fig. 1. It is evident that the large pore volume in support **III** is contained mainly in mesopores of a size between about 100 and 300 Å and that these disappear on impregnation in water solution. The pore size distribution is shown in Fig. 2. The commercial $AlPO_4$ (**III**) shows a clear pore size distribution with a broad two-peak maximum centered around 160 Å.

The cumulative (pore) surface area is plotted against the pore diameter in Fig. 3. The large portion of surface area contained in large pores for the commercial support (**III**) is clearly seen (curve 1). This sample contains about 85% of the total surface area in pores larger than 60 Å. After impregnation with chromium in water solution the same support now has 72% of the total surface area in pores less than 60 Å in diameter (curve 4 in Fig. 3). For supports **I** and **II**

TABLE 2

Pore Volume and Surface Area of Some $AlPO_4$ Samples Measured with the Gravimetric BET Equipment

Sample	Pore volume (cm^3/g)		Cumulative surface area (m^2/g)		BET surface area (m^2/g)
	$P/P_0 < 0.95$	$P/P_0 < 0.99$	$P/P_0 < 0.95$	$P/P_0 < 0.99$	
I	0.247	0.315	127	130	141
II	0.289	0.353	138	142	145
III	1.22	1.27	379	382	350
IIIC	0.197	0.256	107	110	137

the corresponding values are 60 and 52% respectively.

XRD Studies

The fresh $AlPO_4$ supports were studied by XRD, but all three were amorphous with no discrete lines in the diffractogram. To check if the reduced surface area of samples impregnated in water solution was a result of crystallization, the impregnated support **IIIC** was also measured. No discrete diffraction lines were obtained and this sample is also amorphous. It is very likely that the other supports impregnated in water solution are also amorphous.

XPS Studies

The XPS (ESCA) data were quantified for O, Al, P, and Cr. The results are shown in Table 3. The P/Al atom ratio was different for the three different $AlPO_4$ supports. Impregnation resulted in small variations. Preparations based on support **I** gave values of P/Al close to 1.1 and those based on support **II** gave P/Al close to 0.9. In both cases, however, it seems that impregnation in water solution gives a slightly lower P/Al ratio. The commercial $AlPO_4$ gave P/Al ratios close to 1. Larger variations were observed in the Cr/Al atom ratio. The accuracy in determination of Cr $2p$ intensity is not so high since it is obtained from the difference spectra with a larger error (see Fig. 5 below).

However, it was quite obvious that the $AlPO_4$ support **I,** in general, gave a lower Cr/Al atom ratio than the other supports. Possibly, this is caused by the higher phosphorus concentration. The highest Cr/Al ratio is obtained for support **II** with the lowest

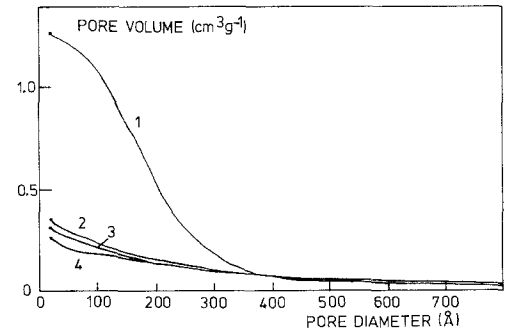

FIG. 1. Cumulative pore volume as a function of the pore diameter for some amorphous $AlPO_4$ samples. (1) support **III,** (2) support **II,** (3) support **I,** and (4) sample **IIIC** (for notation, see text).

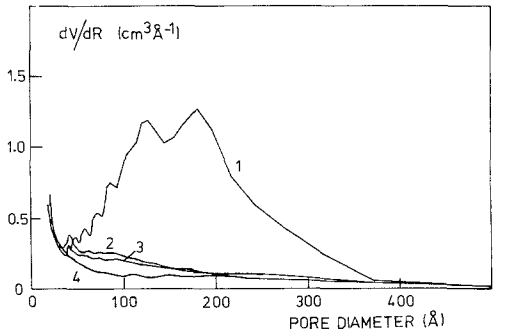

FIG. 2. Pore size distribution for some amorphous $AlPO_4$ samples. Notations are as in Fig. 1.

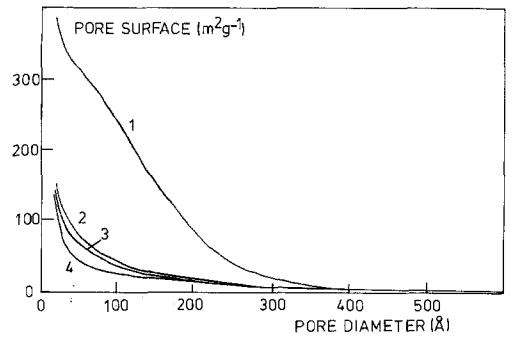

FIG. 3. Cumulative pore surface area as a function of pore diameter for some amorphous $AlPO_4$ samples. Notations are as in Fig. 1.

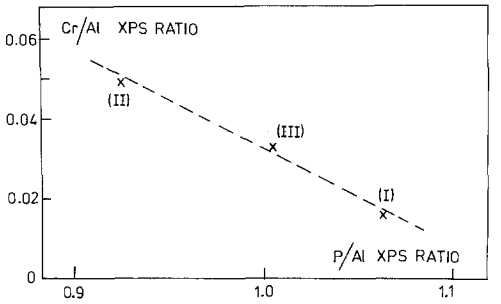

FIG. 4. The Cr/Al atom ratio measured by XPS versus the P/Al atom ratio measured by XPS. The points represent mean values for series **I, II,** and **III,** respectively.

P/Al ratio. Figure 4 shows the linear correlation between the Cr/Al and the P/Al mean values for all three supports. This means that on a support with a high P/Al much of the chromium is not deposited on the surface in dispersed form, but as larger particles, perhaps as chromium phosphate.

The various core lines investigated for the different samples were very similar, and all appeared as single lines. Table 4 shows the O 1*s*, Al 2*p*, and P 2*p* bond energies (BE). The Cr 2*p* core line is interfering with the O 1*s* electron loss background, which contains a certain structure with a maximum around 580 eV. Due to the low Cr concentration pure Cr 2*p* spectra could not therefore be obtained. Figure 5 shows some difference spectra of Cr 2*p* calculated by subtracting spectra for the pure support from those containing chromium. The Cr $2p_{3/2}$ BE obtained is about 578 eV. Charging effects were arbitrarily adjusted for by giving the O 1*s* core line a BE of 531.9 eV. The C 1*s* line could not be used for this purpose since the various samples did not seem to contain identical carbon species. Comparison of the Cr $2p_{3/2}$ BE values obtained here with the literature values is thus not quite straightforward. However, chromium(III) as in Cr_2O_3 gives a BE of 576.2 to 576.8 eV (*20–25*), if referenced to Au $4f_{7/2}$ BE = 84.0 eV or C 1s BE

TABLE 3

Atom Ratios in $AlPO_4$ Samples Measured by XPS

Sample	O/Al	P/Al	Cr/Al
I	5.9[a]	1.07	—
IA	6.1[a]	1.10	0.026
IB	5.8[a]	1.06	0.013
IC	5.6[a]	1.02	0.010
II	6.3	0.93	—
IA	6.4	0.93	0.042
IIB	6.4	0.93	0.063
IIC	6.4	0.91	0.043
III	6.8	1.01	—
IIIA	6.7	0.97	0.033
IIIB	6.8	1.02	0.025
IIIC	6.6	1.02	0.040

[a] Measured at a transmission different from that for supports **II** and **III**.

TABLE 4

Binding energies (BE)[a] and Half-Widths[b] for Some Core Lines Measured for the Various $AlPO_4$ Samples

Sample	O 1*s*	Al 2*p*	Al 2*s*	P 2*p*	P 2*s*	Cr $2p_{3/2}$
I	531.9	74.7	119.5	134.1	191.4	—
	(2.6)	(2.7)	(3.0)	(2.6)	(3.2)	
IA	531.9	74.8	119.6	134.2	191.5	577.6
	(2.6)	(2.4)	(2.9)	(2.6)	(3.1)	
III	531.9	74.8	119.6	134.1	191.4	—
	(2.7)	(2.4)	(2.7)	(2.6)	(3.2)	
IIIA	531.9	74.8	119.6	134.1	191.4	578.2
	(2.6)	(2.3)	(2.7)	(2.5)	(3.1)	
IIIC	531.9	74.7	119.5	134.1	191.4	577.9
	(2.6)	(2.4)	(3.0)	(2.6)	(3.1)	

[a] Corrected for charging effects with O 1*s* = 531.9 eV.
[b] Within parenthesis.

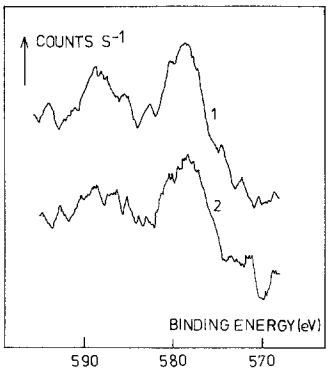

FIG. 5. Cr 2*p* spectra for some chromium-impregnated $AlPO_4$ samples. The spectra are smoothed by a 39-point quadratic smoothing. (1) Support **II** impregnated with $Cr((H_2O)_4Cl_2)Cl$ in water (sample **IIC**). (2) Support **III** (Grace) impregnated with $Cr(acac)_3$ in ethanol (sample **IIIA**).

= 285.0 eV. For chromium(VI) as in CrO_3 and chromates and dichromates BE values are 579.1 to 580.3 eV (*20–25*), based on the same reference. Our values of about 578 eV are intermediate between these two. It has, however, been reported that chromium supported on silica gel gives a Cr $2p_{3/2}$ BE shifted about 1.4 eV toward higher BE compared to the corresponding bulk oxides. Thus our Cr BE of about 578 eV corresponds well with the presence of chromium(III) species, by comparison with 576.6 eV for Cr_2O_3. It has been reported that for calcination temperatures above 500°C, chromium(III) states are dominating (*26*).

FTIR Spectra of Hydroxyl Groups

Figure 6 shows the FTIR spectra of surface hydroxyl groups on the three amorphous $AlPO_4$ supports. Support **I** (Fig. 6A) shows two IR bands at 3793.8 and 3768.5 cm^{-1} at room temperature (spectrum 1). After cooling to −85°C these bands are shifted to higher wavenumbers by 4.4 and 5.0 cm^{-1} (spectrum 2) and their intensity increases. Cooling even more to −115°C (spectrum 3) does not yield additional changes. Figure 6B shows that the support **II** gives the same IR bands from surface hydroxyl groups as support **I** with similar shifts on cooling to low temperatures, but the relative intensities of the two bands have changed, the IR band at 3768.5 cm^{-1} being much smaller in Fig. 6B. Support **III** (Fig. 6C) shows a small, additional IR band from surface hydroxyl groups at 3743.2 cm^{-1}, which shifts at lower temperatures by only 2.4 cm^{-1} and is barely noticeable in Figs. 6A and 6B. The intensity of this IR band does not increase on cooling to lower temperatures (spectra 2 and 3 in Fig. 6C). The IR band at 3795 cm^{-1} has been assigned in the literature (*4*) to aluminum surface hy-

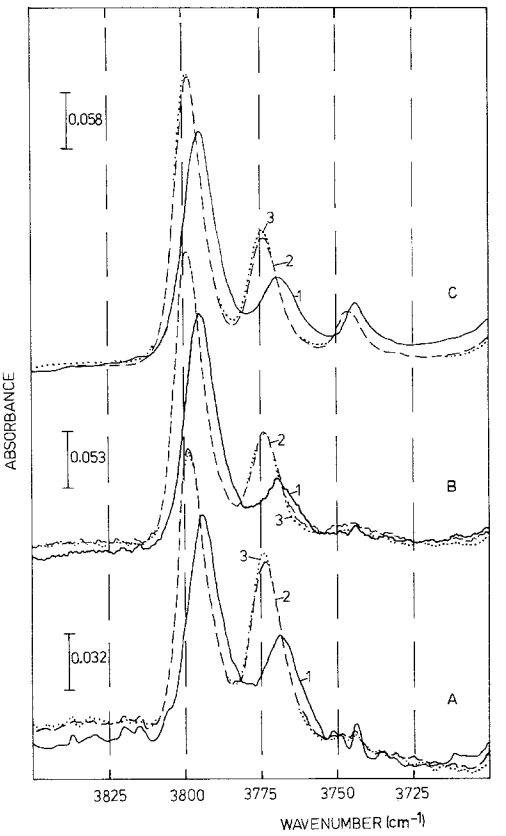

FIG. 6. FTIR spectra of the stretching vibration of surface AlO–H groups of amorphous $AlPO_4$ after evacuation at 800°C. (A) Spectra with support **I** (P/Al ratio, 1.1). Spectrum 1 was recorded with 10 kPa CO at room temperature, and spectrums 2 and 3 were recorded with 100 Pa CO at −85 and −115°C, respectively. (B) Similar spectra with support **II** (P/Al ratio, 0.9) and (C) spectra with support **III**.

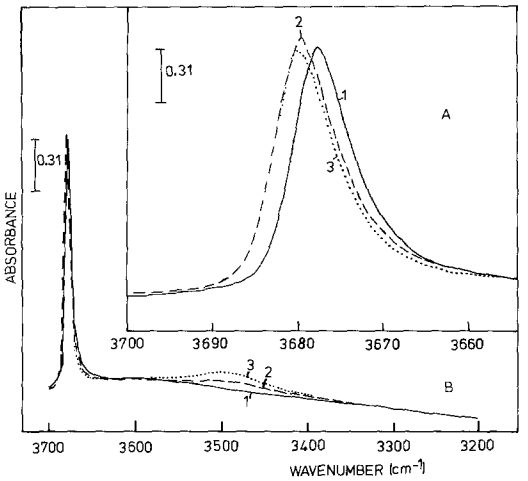

FIG. 7. FTIR spectra of the stretching vibration of surface PO–H groups of amorphous $AlPO_4$ after evacuation at 800°C using support **II** (P/Al ratio, 0.9). Spectrum notation as in Fig. 6. It should be noted that different wavenumber scales have been used for (A) and (B).

droxyl groups and this assignment will also be used for the other two IR bands. Curiously, the difference between the first and the second of these IR bands is exactly the same as that between the second and the third (25.3 cm^{-1}). This is evidence for a consecutive addition of a similar ligand to the aluminum ion. This ligand is most probably an oxygen ion and the coordination number of the aluminum will be raised to five and six, respectively.

Figure 7A shows the FTIR spectra of the phosphorus surface hydroxyl group (*4*). At room temperature (spectrum 1) this IR band is at 3677.5 cm^{-1} on support **II.** On cooling to 85°C a shift to higher wavenumbers by 2.0 cm^{-1} was observed in spectrum 2, but in contrast to IR bands in Fig. 6, no intensity increase of the already very large IR band was observed. Instead, the intensity of this band decreases on further cooling to −115°C (spectrum 3 in Fig. 7A). Similar spectra were obtained with the other two supports and are therefore not shown here. Figure 7B gives a clue to why the IR band from the phosphorus surface hydroxyl groups does not increase with lower temperature. A broad new band is formed at 3495.6 cm^{-1}. Obviously a part of the IR band at 3677.5 cm^{-1} is converted to a new IR band at much lower wavenumbers. A possible candidate for such a conversion is the adsorption of CO at low temperatures. Cooling the samples in the presence of Ar did show the small shifts to higher wavenumbers in the IR spectra of the surface hydroxyl groups, but not the large one of the phosphorus hydroxyl group from 3677.5 to 3495 cm^{-1}.

In Fig. 8 the IR band from the stretching vibration of adsorbed CO is at 2170.1 cm^{-1}. It can be clearly seen that this IR band also grows with decreasing temperature and is not observed at room temperature.

A CO absorption band similar to that at 2170.1 cm^{-1} is known for CO adsorbed on surface silanol groups on silica gel (*27*) where the free hydroxyl group has a band around 3751 cm^{-1}, which is shifted to 3673 cm^{-1} ion adsorption of CO and the new CO IR band from adsorbed CO is observed at 2157 cm^{-1}. One can notice an opposite trend for the stretching vibration of the free surface hydroxyl groups and that of the adsorbed CO. A CO absorption on the aluminum surface hydroxyl groups at 3793.8 and

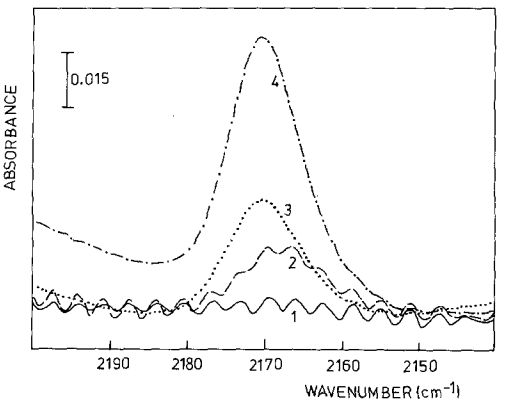

FIG. 8. FTIR spectra of the stetching vibration of CO adsorbed on amorphous $AlPO_4$ (support **II**) at room temperature and 10 kPa CO (spectrum 1), at −50°C and 10 kPa CO (spectrum 2), at −85°C and 100 Pa CO (spectrum 3), and at −115°C and 100 Pa CO (spectrum 4).

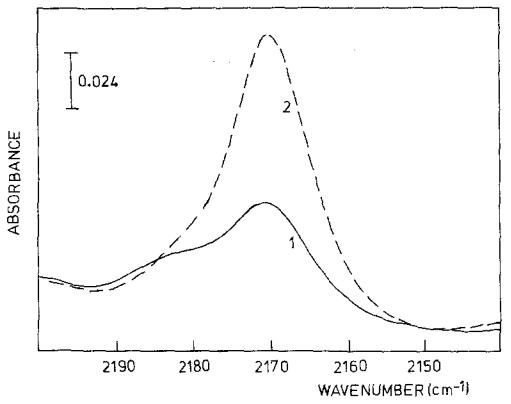

FIG. 9. FTIR spectra of the stretching vibration of CO adsorbed on amorphous $AlPO_4$ (support **III**) at −85°C and 100 Pa CO (spectrum 1) and at −115°C and 100 Pa CO (spectrum 2).

3768.5 cm^{-1} was not observed and is most probably too weak for the experimental conditions used in this work. The aluminum hydroxyl group with the IR band at 3743.2 cm^{-1} is not increasing in intensity on cooling and does most likely adsorb CO. Because the hydroxyl stretching vibration of this AlO–H group is at 3743.2 cm^{-1}, similar to that of silanol groups at 3751 cm^{-1}, the new IR band from adsorbed CO would be expected near 2157 cm^{-1}. This band, however, is most probably too weak to be noticed in the CO spectra.

Figure 9 shows the FTIR spectra of CO adsorbed on surface hydroxyl groups using support **III.** One can notice that the CO IR band has become asymmetric through a shoulder at 2182.8 cm^{-1}, which is not observed using the other two supports. Although the CO causing this IR band cannot be adsorbed on the aluminum surface group with the IR band at 3743.2 cm^{-1}, because that would be expected around 2157 cm^{-1} (see above), a structural difference in the support **III** compared to the other two supports may be the origin of both phenomena.

A CO IR band at 2200 cm^{-1} from CO adsorbed on aluminum surface ions with a coordination number of four was noticed in CO IR spectra from all supports, but none was noticed at 2228 cm^{-1} for three-coordinated Al surface ions. The latter band is found on silica gel modified with aluminum oxide.

DISCUSSION

As already stated above, the amorphous $AlPO_4$ is structurally very similar to amorphous silica gel because both are built with tetrahedral MO_4 units. This simple model, however, does not include all the results observed above (e.g., several aluminum surface hydroxyl groups) and must consequently be modified.

Surface hydroxyl groups with Al, Si, and P show an increasing acidity and a decreasing O–H stretching vibration. The three elements also show an increasing electronegativity (*28*). Plotting the electronegativity over the stretching vibration of the surface hydroxyl groups gives a nearly perfect linear relation, as shown in Fig. 10. This is even valid after inclusion of amorphous boron phosphates, which have surface hydroxyl groups at 3696 and 3664 cm^{-1} (assigned to BOH and POH groups, respectively) (*29*). In view of the other aluminum surface hydroxyl groups at 3768.5 and 3743.5 cm^{-1}, which do not fit into the linear correlation in Fig. 10, we restrict the linear relation between the electronegativity of the elements

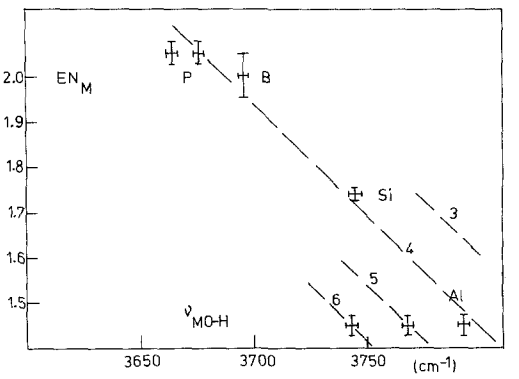

FIG. 10. The electronegativity of elements B, Al, Si, and P plotted against the stretching vibration of single surface hydroxyl groups of these elements in amorphous metal phosphates.

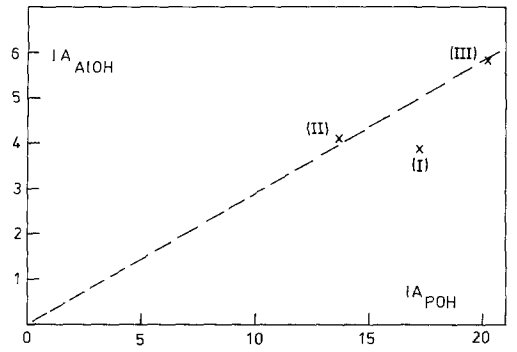

FIG. 11. The integrated absorbance of the stretching vibrations from single surface AlOH groups plotted against that from single surface POH groups. The ratio of the integrated absorbance characterizes the surface of amorphous aluminum phosphates.

and the stretching vibration and Brønsted acidity of its surface hydroxyl group to a coordination number of *four* (tetrahedral coordination). This relation may now provide a tool to assign coordination numbers to surface metal ions through the IR bands of the stretching vibration of their surface hydroxyl groups.

We therefore assign the two other AlOH IR bands at 3768.5 and 3743.5 cm^{-1} to aluminum surface species with increasing coordination number, i.e., five and six. In Fig. 10 two tentative, dashed lines are drawn through these points parallel to the main line. We do not know at present if a linear relation also holds for the other coordination numbers five and six (and possibly also three). This hypothesis will be investigated by us in further studies and it is hoped that more data points will be added to the picture.

The integrated absorbance of the aluminum surface hydroxyl groups is plotted against that of the phosphorus surface hydroxyl groups in Fig. 11. One should notice that these data points represent ratios, which means that experimental errors due to different sample disk positions and different sample disk thickness cancel each other. The data points give a straight line for supports **II** and **III.** This line goes through the origin in Fig. 11. Support **I** deviates from this line, which means that the ratio of AlOH and POH groups is different for this support than for the other two. Comparing the points for supports **II** and **III** with values for the specific surface area (Table 1), one notices that the specific surface area increases much more than the integrated absorbance of the surface hydroxyl groups. This means that building units other than tetrahedra are present on the surface of support **III.**

These will most probably be aluminum–oxygen octahedra. First, the two additional aluminum surface hydroxyl groups can be explained by assumming additional oxygen ligands at the aluminum ion so that five- and six-coordinated aluminum surface ions are formed; second, the additional IR band from adsorbed CO at 2182.5 cm^{-1} is close to that observed on five-coordinated, coordinatively unsaturated surface aluminum cations on silica gel at 2170 cm^{-1} (*30*). Coordinatively unsaturated aluminum surface cations with a coordination number of four, which are Lewis acids and adsorb CO with IR bands at 2200 (2190) cm^{-1} (*30*), are observed on aluminum phosphates. Strong Lewis acids, which give a CO IR band at 2228 cm^{-1} assigned to CO on three-coordinated aluminum ions, are not observed on amorphous $AlPO_4$. Such aluminum surface ions are, however, present on Al_2O_3/silica gel catalysts in large numbers and their absence may be the cause of the poor catalytic activity of aluminum phosphates in hydrocarbon conversions (*4*).

Coordination numbers higher than four are excluded for silicon in silica gel. One can therefore conclude that amorphous aluminum phosphates not only have different surface hydroxyl groups compared to silica gel, but also are structurally different from silica gel on the atomic scale.

The linear relation in Fig. 10 can be interpreted as due to an electron drawing effect from the surface cation M, so that the O–H bond becomes weaker and more ionic with decreasing electron density on the oxygen atom. The latter conclusion means that the

dipole moment of the O–H bond increases as well as, indirectly, the integrated intensity of the O–H stretching vibration. With the assumption that the same amounts of AlOH and POH groups are present on the surface of supports **II** and **III**, we can derive from Fig. 11 a factor of roughly 3 per 100 cm^{-1} for the increase in the integrated intensity versus the shift of the OH surface groups. Applying this correction we can deduce that roughly 68, 30, and 2% (support **I**), 79, 18, and 3% (support **II**), and 71, 20, and 9% (support **III**) of the aluminum surface atoms are present as four-, five-, and six-coordinated species, respectively.

ACKNOWLEDGMENTS

This work has been supported by the Swedish Board for Technical Development (STU) and the National Energy Administration (SEV).

REFERENCES

1. Moffat, J. B., *Catal. Rev.-Sci. Eng.* **18,** 199 (1978).
2. O'Keeffe, M., and Hyde, B. G., *Acta Crystallogr.* **65,** 27 (1978).
3. Iler, R. K., "The Chemistry of Silica," pp. 660 et seq. Wiley, New York, 1979.
4. Peri, J. B., *Discuss. Faraday Soc.* **52,** 55 (1971).
5. McDaniel, M. P., and Johnson, M. M., *J. Catal.* **101,** 446 (1986).
6. Cheung, T. T. P., Willcox, K. W., McDaniel, M. P. Johnson, M. M., Bronniman, C., and Frye, J., *J. Catal.* **102,** 10 (1986).
7. Freeman, W. J., Wilson, D. R., Ernst, R. D., Smith, P. D., Klendworth, D. D., and McDaniel, M. P., *J. Polym. Sci., Poly. Chem. Ed.* **25,** 2063 (1987).
8. McDaniel, M. P., *Ind. Eng. Chem. Res.* **27,** 1559 (1988).
9. McDaniel, M. P., Leigh, C. H., and Wharry, S. M., *J. Catal.* **111,** 170 (1989).
10. Clark, A., Hogan, J. P., Banks, R. L., and Lanning, W. C., *Ind. Eng. Chem.* **48,** 1152 (1956).
11. Karol, F. J., Karapinka, G. L., Wu, C., Dow, A. W., Johnson, R. N., and Carrick, W. L., *J. Polym. Sci., Poly. Chem. Ed.* **10,** 2621 (1972).
12. Rebenstorf, B., and Larsson, R., *Z. Anorg. Allg. Chem.* **478,** 119 (1981).
13. Rebenstorf, B., and Larsson, R., *J. Mol. Catal.* **11,** 247 (1981).
14. Rebenstorf, B., *Z. Anorg. Allg. Chem.* **513,** 103 (1984).
15. Rebenstorf, B., *J. Mol. Catal.* **45,** 263 (1988).
16. Rebenstorf, B., *J. Mol. Catal.* **56,** 170 (1989).
17. Rebenstorf, B., and Lindblad, T., *Acta Chem. Scand.,* **44,** 789 (1990). [Part 1 of this series]
18. Dollimore, C. D., and Heal, G. R., *J. Appl. Chem.* **14,** 109 (1964).
19. Rebenstorf, B., and Larsson, R., *Z. Anorg. Allg. Chem.* **453,** 127 (1979).
20. Schreifels, J. A., Rodero, A., and Swartz, W. E., Jr., *Appl. Spectrosc.* **33,** 380 (1979).
21. Wichterlova, B., Krajcikova, L., Tvaruzkova, Z., and Beran, S., *J. Chem. Soc., Faraday Trans. 1* **80,** 2639 (1984).
22. Okamoto, Y., Fujii, T., Imanaka, T., and Teranishi, S., *Bull. Chem. Soc. Japan* **49,** 859 (1976).
23. Cimino, A., De Angelis, B. A., Luchetti, A., and Minelli, G., *J. Catal.* **45,** 316 (1976).
24. Allen, G. C., Curtis, M. T., Hooper, A. J., and Tucker, P. M., *J. Chem. Soc., Dalton Trans.* 1675 (1973).
25. Merryfield, R., McDaniel, M. P., and Parks, G., *J. Catal.* **77,** 348 (1982).
26. Best, S. A., Squires, R. G., and Walton, R. A., *J. Catal.* **47,** 292 (1977).
27. Ugliengo, P., Saunders, V. R., and Garrone, E., *J. Phys. Chem.* **93,** 5210 (1989).
28. Kneen, W. R., Rogers, M. J. M., and Simpson, P., "Chemistry," p. 797. Addison–Wesley, London, 1972.
29. Moffat, J. B., and Neeleman, J. F., *J. Catal.* **34,** 376 (1974).
30. Rebenstorf, B., and Andersson, S. L. T., *J. Chem. Soc., Faraday Trans. 1,* **86,** 3153 (1990).